PERGAMON

Available online at www.sciencedirect.com

SCIENCE DIRECT®

Polyhedron 22 (2003) 1809–1816

POLYHEDRON

www.elsevier.com/locate/poly

A stable organic triradical with truncated π-conjugation as a model for single-component organic molecule-based ferrimagnetics

Chika Kaneda [a], Daisuke Shiomi [a], Kazunobu Sato [b], Takeji Takui [b,*]

[a] Department of Materials Science, Graduate School of Science, Osaka City University, Sugimoto 3-3-138, Sumiyoshi-ku, Osaka 558-8585, Japan
[b] Department of Chemistry, Graduate School of Science, Osaka City University, Sugimoto 3-3-138, Sumiyoshi-ku, Osaka 558-8585, Japan

Received 6 October 2002; accepted 12 December 2002

Abstract

As a novel molecular design for genuinely organic molecule-based ferrimagnets, we have proposed a strategy of 'single-component ferrimagnetics.' When a π-biradical with an $S = 1$ ground state and a π-monoradical with $S = 1/2$ are united by σ-bonds, the π-conjugation between the biradical and the monoradical moieties should be truncated in the resultant triradical. This gives magnetic degrees of freedom for both $S = 1$ and $S = 1/2$ in the single molecule, serving as a building block for organic molecular ferrimagnets. We have designed and synthesized a triradical, 2,2,6,6-tetramethyl-pipelidine-1-*N*-oxyl-4-carboxylic acid 2,4-bis(1-oxyl-3-oxido-4,4,5,5-tetramethyl-2-imidazolin-2-yl)-phenyl ester (**2**) as a model compound for single-component ferrimagnetics. Solution-phase ESR spectra from **2** are explained by a perturbation treatment assuming that the exchange interaction within the biradical moiety is much larger than those between the biradical and the monoradical moieties, which is suitable for single-component ferrimagnetics. From susceptibility measurements for a cyclohexane-substituted biradical, cyclohexane carboxylic acid 2,4-bis(1-oxyl-3-oxido-4,4,5,5-tetramethyl-2-imidazolin-2-yl) phenyl ester (**4**) as a biradical analogue of **2**, it is shown that the intramolecular ferromagnetic interaction has been found to be unaffected by the chemical modification for anchoring the monoradical moiety.
© 2003 Elsevier Science Ltd. All rights reserved.

Keywords: Single-component organic ferrimagnet; Magnetic susceptibility; Electron spin resonance; Nitronyl nitroxide; Perturbation treatment; Triradical

1. Introduction

More than 30 ferromagnets have been documented as genuinely organic molecule-based materials [1] after the discovery of the first genuinely organic ferromagnet [2]. Molecule-based ferrimagnets have also been attracting attention as one of the seemingly facile approaches to organic magnets after the first Buchachenko's proposal in 1979 [3]. Ferrimagnetic spin alignment is conventionally regarded as an antiparallel coupling of different spin quantum numbers, e.g., $S = 1$ and $S = 1/2$, giving net and bulk magnetization. This classical picture has been initiated by Néel in his mean field theory [4]. Organic ferrimagnetics is customarily based on the tendency for organic open-shell molecules to have antiferromagnetic intermolecular interactions. The antiferromagnetic interactions would bring about the antiparallel spin alignment between neighboring molecules with different magnetic moments to result in a possible ordered state. Genuinely organic ferrimagnets composed of discrete, two kinds of organic open-shell molecules, however, have not been discovered yet. The organic ferrimagnets have been a challenging and long-standing issue in materials science. The possible occurrence of the ferrimagnetic spin alignments in organic molecular assemblages has been examined by the authors both from experiments and theoretical calculations in quantum terms [5].

A practical and inevitable difficulty in constructing molecule-based crystalline ferrimagnetics is separative crystallization from solutions of molecules with different spin quantum numbers. Co-crystallization of distinct

* Corresponding author. Tel.: +81-6-6605-2605; fax: +81-6-6605-3137.
E-mail address: takui@sci.osaka-cu.ac.jp (T. Takui).

0277-5387/03/$ - see front matter © 2003 Elsevier Science Ltd. All rights reserved.
doi:10.1016/S0277-5387(03)00151-7

molecules in a crystalline solid state generally gives rise to a decrease in entropy, preventing the molecules from packing in a structurally ordered fashion. Competitive attractive forces between the molecules are needed to overcome the separative crystallization driven by entropy. As a purposive molecular design for purely organic molecule-based ferrimagnets, the authors have proposed a strategy of 'single-component ferrimagnetics' [6,7], which is schematically shown in Fig. 1. When a π-biradical with $S = 1$ ground state and a π-monoradical with $S = 1/2$ are united by σ-bonds, the π-conjugation between the biradical and the monoradical moieties should be truncated in the resultant triradical molecule. The σ-bonds serve as an ultimate attractive force between the π-conjugated molecules and give the triradical the magnetic degrees of freedom for both $S = 1$ and $S = 1/2$ in the single molecule. Antiferromagnetic interactions underlying the ferrimagnetic spin alignment of $S = 1$ and $S = 1/2$ should be operative via an *intermolecular* π–π orbital overlap between π-SOMO's of the constituent biradical and monoradical moieties in head-to-tail molecular packings such as depicted in Fig. 1(c) and (d). The intermolecular antiferromagnetic interaction denoted by J_{AF} in the figure affords the ferrimagnetic spin alignment.

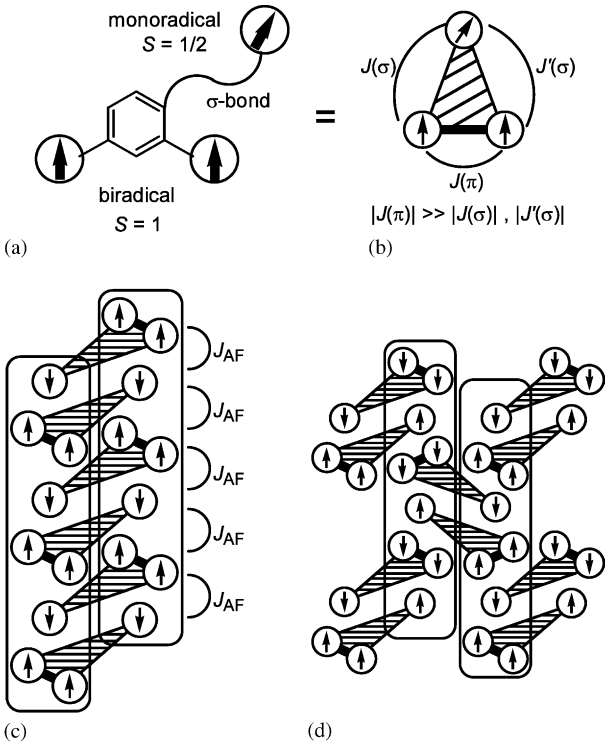

Fig. 1. A triradical consisting of weakly coupled biradical and monoradical moieties as a building block of single-component ferrimagnetics. (b) A schematic picture of the three-centered exchange-coupled system. $J(\pi)$ denotes the intramolecular exchange interaction within the biradical moiety, which is coupled with the monoradical moiety by $J(\sigma)$ and $J'(\sigma)$ ($|J(\sigma)| \sim |J'(\sigma)| \ll |J(\pi)|$). (c, d) Examples of the ferrimagnetic chain based on the intermolecular antiferromagnetic interaction J_{AF} in a crystalline solid state. The rounded rectangles represent the alternating molecular chain of the biradical and the monoradical moieties.

The σ-bonds should play a role of uniting the two molecular moieties only. If the additional intramolecular interactions through the σ-bonds $|J(\sigma)|$ and $|J'(\sigma)|$ (Fig. 1) are in the same order of magnitude as the ferromagnetic interaction $J(\pi)$ in the biradical moiety, we acquire no more than assemblages of triradical molecules in a doublet ($S = 1/2$) or a quartet ($S = 3/2$) state, depending on signs of $J(\sigma)$ and $J'(\sigma)$. Therefore, in the single-component ferrimagnetics it is vitally important whether or not the interactions $J(\sigma)$ and $J'(\sigma)$ are negligible as compared with $J(\pi)$. We have synthesized a triradical **1** as a building block for single-component ferrimagnetics [7]. The magnitude of $|J(\sigma)|/k_B$ and $|J'(\sigma)|/k_B$ in **1** has been found to be about 100 mK, which is much weaker than $J(\pi)/k_B \sim 10$ K [6,7]. For the triradical **1**, an intermolecular ferrimagnetic short-range ordering has been found to develop along a one-dimensional molecular chain of the type shown in Fig. 1(d). The interactions $J(\sigma)$ and $J'(\sigma)$ in **1**, however, act as interchain couplings, as depicted in Fig. 1(d) and fall within the same order as those of the intermolecular interactions along the chain, giving rise to an antiparallel coupling between the chains [7]. Further suppression of the magnitude of $J(\sigma)$ and $J'(\sigma)$ should be promising for the final goal of a three-dimensional ferrimagnetic ordering.

In this study, we have designed and synthesized a TEMPO-based triradical **2** (Fig. 2). The phenyl nitronyl nitroxide in the monoradical moiety of **1** is replaced by an aliphatic ring of TEMPO radical in **2**. The π-conjugation in **2** is expected to be more efficiently truncated in the aliphatic-substituted monoradical than in **1**. We invoke hyperfine ESR spectroscopy in fluid

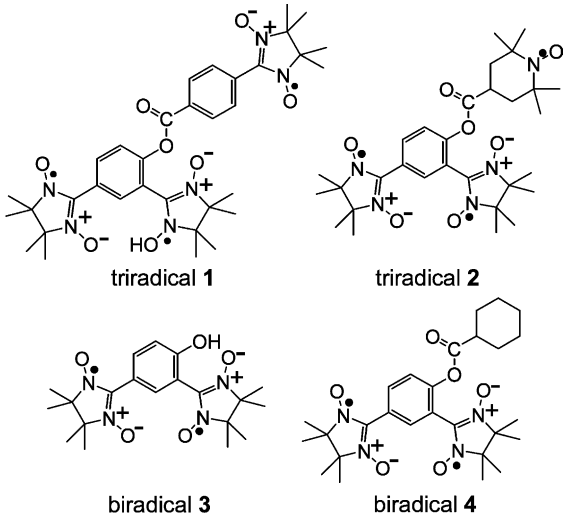

Fig. 2. Biradicals and triradicals as building blocks of single-component ferrimagnetics.

solutions as a probe for traces of exchange couplings $J(\sigma)$ and $J'(\sigma)$ in **2**, the magnitude of which is expected to be outside the range for conventional susceptibility measurements. Exchange-coupled hyperfine ESR spectroscopy is revived in terms of molecule-based magnetics. A perturbation treatment of the exchange couplings gives a rationale to the observed hyperfine ESR spectra from **2** and can afford to estimate for the magnitude of $J(\sigma)$ and $J'(\sigma)$. The intramolecular interaction of the parent biradical **3** has been known to be $J(\pi)/k_B = 13$ K [8]. Cyclohexane-substituted biradical **4** is also investigated as a biradical analogue of **2** in order to confirm that the intramolecular exchange interaction in **3** remains unaffected by the esterification.

2. Experimental

The TEMPO-substituted triradical **2** was synthesized by the esterification of the parent phenol biradical **3** [8] and 4-carboxy TEMPO with dicyclohexylcarbodiimide in dichloromethane, followed by recrystallization from an ethyl acetate solution. The cyclohexyl biradical **4** was synthesized from **3** and cyclohexane carboxylic acid in the same way as **2**. The biradical **4** was chromatographed on silicagel using acetone-ether of 1:10 volume ratio as an eluent.

The ESR spectra were recorded in toluene solutions, which were degassed by a freeze-pump-thaw cycle and sealed in vacuo, using a JEOL X-band spectrometer JES-FE2XG in the temperature range of 200–320 K. The concentration of the solution was 1×10^{-5} mol dm^{-3}. The magnetic susceptibility was measured for powder samples on a Quantum Design SQUID Magnetometer MPMS-XL with an applied field of 0.1 T in the temperature range of 1.9–298 K.

3. Results and discussion

3.1. Magnetic properties of cyclohexyl biradical *4*

Temperature dependence of paramagnetic susceptibility χ_p of **4** is shown in Fig. 3. On lowering the temperature, the $\chi_p T$ value increases, indicating that the intramolecular ferromagnetic interaction in the parent phenol biradical **3** is retained in **4**. The $\chi_p T$ value decreases below 10 K, as depicted in Fig. 3, and the decrease is attributed to intermolecular antiferromagnetic interactions. The temperature dependence of $\chi_p T$ is analyzed in terms of the thermal equilibrium between the singlet ($S = 0$) and triplet ($S = 1$) states within the molecule (the modified Bleany–Bowers equation [9]),

$$\chi_p = \frac{2N_A g^2 \mu_B^2}{k_B(T - \theta)} \frac{1}{3 + \exp(-2J(\pi)/k_B T)} \alpha \quad (1)$$

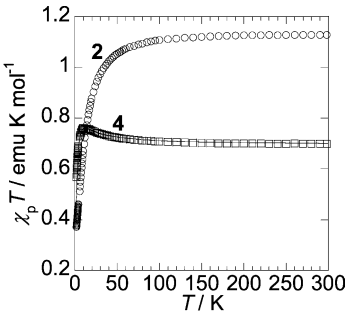

Fig. 3. Paramagnetic susceptibility χ_p of the triradical **2** (the circles) and the biradical **4** (the squares) in the $\chi_p T$ vs. T plots. The solid line is calculated from Eq. (1) with the intramolecular exchange interaction of $J(\pi)/k_B = 8.2$ K and the intermolecular mean field of $\theta = -1.5$ K.

where the parameter $J(\pi)$ denotes the intramolecular exchange interaction in the π-conjugation of the *m*-phenylene skeleton in **4** defined by the Heisenberg spin Hamiltonian,

$$H = -2J(\pi)\mathbf{S}_1 \cdot \mathbf{S}_2 \quad (2)$$

of $S_1 = S_2 = 1/2$. The intermolecular interaction is approximated by the mean field θ in Eq. (1). The parameter α stands for the purity of the sample. The other symbols have their usual meanings. The model reproduces the experimental $\chi_p T$ values with $J(\pi)/k_B = 8.2$ K, $\theta = -1.5$ K, $\alpha = 0.92$, and the *g*-factor of $g = 2.007$, as shown by the solid curve in the figure. The ferromagnetic interaction is found to be retained after the esterification.

3.2. Hyperfine ESR spectra of TEMPO-based triradical *2*

3.2.1. Exact diagonalization of the spin Hamiltonian

The hyperfine ESR spectra from the triradical **2** in the toluene solution are shown in Fig. 4(a). An intense triad of signals with spacings of the ^{14}N hyperfine coupling, 1.38 mT, of the TEMPO monoradical feature in the spectra. The other signals between the triad decrease in intensity on lowering the temperature, as shown in the figure. The hyperfine splitting patterns of the triradical were analysed in terms of the spin Hamiltonian,

$$\begin{aligned} H = {} & g\mu_B B(S_{b1}^z + S_{b2}^z + S_m^z) - 2J(\pi)\mathbf{S}_{b1} \cdot \mathbf{S}_{b2} \\ & -2J(\sigma)\mathbf{S}_m \cdot \mathbf{S}_{b1} - 2J'(\sigma)\mathbf{S}_{b2} \cdot \mathbf{S}_m \\ & +A_b(I_{b1}^z S_{b1}^z + I_{b2}^z S_{b2}^z) + A_m I_m^z S_m^z \end{aligned} \quad (3)$$

which consists of the electronic Zeeman, the three-centered Heisenberg exchange ($S_{b1} = S_{b2} = S_m = 1/2$), and the hyperfine coupling terms. The Hamiltonian is schematically shown in Fig. 5. The parameters A_b and A_m denote the isotropic hyperfine coupling constants for the biradical and monoradical moieties, respectively. The additional exchange interactions through the σ-bonds are represented by $J(\sigma)$ and $J'(\sigma)$. B denotes the

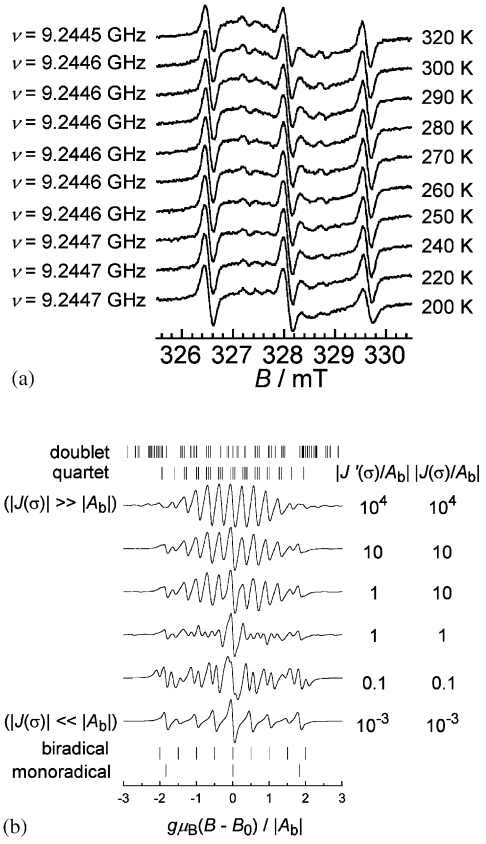

Fig. 4. ESR spectra of the triradical **2**. (a) Recorded in a toluene solution. ν stands for the microwave frequency. (b) Simulated by the exact diagonalization of the spin Hamiltonian Eq. (3). B_0 stands for the central field, $B_0 = h\nu/g\mu_B$. The sticks in the upper portion indicate the resonance field for the quartet and doublet states of the triradical in the strong exchange limit ($|J(\sigma)| \gg |A_b|$), while in the lower portion are shown those of the constituent biradical and monoradical in the weak exchange limit ($|J(\sigma)| \ll |A_b|$).

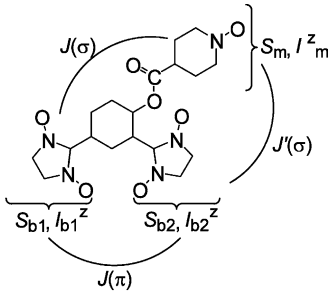

Fig. 5. Schematic drawing for the spin Hamiltonian, Eq. (3). The nuclear spin operators for the nitrogen nuclei in the nitronyl nitroxide groups are given by $I^z_{b1} \equiv I^z_{b1}(1) + I^z_{b1}(2)$ and $I^z_{b2} \equiv I^z_{b2}(1) + I^z_{b2}(2)$.

static magnetic field. The nuclear spin operators for the nitrogen nuclei in the nitronyl nitroxide groups are given by

$$I^z_{b1} \equiv I^z_{b1}(1) + I^z_{b1}(2) \quad (4)$$

$$I^z_{b2} \equiv I^z_{b2}(1) + I^z_{b2}(2) \quad (5)$$

In Eq. (3), the hyperfine interctions are assumed to be small as compared with the electronic Zeeman interaction and nonsecular terms of the hyperfine coupling are neglected. The hyperfine term in Eq. (3) does not commute with the exchange term. Therefore, the energy eigenvalues and the spin eigenfunctions of the spin Hamiltonian, hence the resonance field and intensity of hyperfine ESR transitions, depend on the relative magnitudes of the exchange interactions and the hyperfine interactions. The magnitude of hyperfine interaction $|A|$ falls within the order of 1 mT (1 mK or 10^{-3} cm^{-1} for $g = 2$) for nitrogen nuclei in stable nitroxide radicals. It is feasible to determine the magnitude of exchange interaction in this range of energy in terms of hyperfine ESR spectroscopy. Thus, the hyperfine splitting patterns of organic oligo- or poly-radicals are a spectroscopic 'probe' for intramolecular exchange interactions within the molecules [10].

The resonance fields and the transition probabilities were calculated from the exact numerical diagonalization of the spin Hamiltonian Eq. (3). The Hamiltonian is represented by a $2^3 \times 2^3$ matrix in the ket space spanned by the set of the direct products,

$$S^z_I|m^S_{b1},\ m^S_{b2},\ m^S_m,\ m^I\rangle = \pm 1/2|m^S_{b1},\ m^S_{b2},\ m^S_m,\ m^I\rangle \quad (I = b1,\ b2,\ m) \quad (6)$$

where m^I is the collective index for a nuclear spin configuration,

$$m^I = \{m_{b1}(1),\ m_{b1}(2),\ m_{b2}(1),\ m_{b2}(2),\ m_m\} \quad (7)$$

The Hamiltonian affords one quartet and two doublet

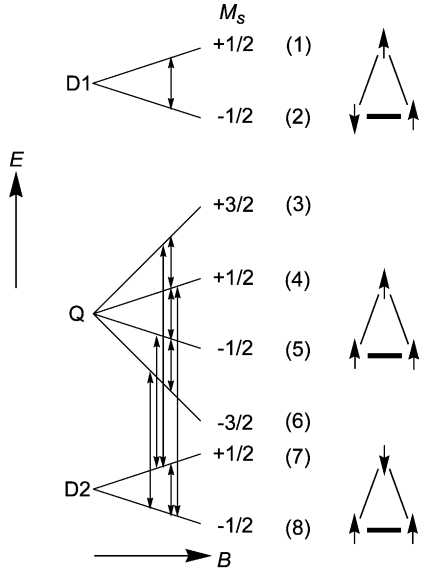

Fig. 6. Energy diagram for the triradical **2**. The Zeeman sublevels are designated by the quantum numbers M_S of the total spin and the numbers in the parentheses, which correspond to those listed in Table 1. The arrows indicate the allowed ESR transitions. The hyperfine sublevels are omitted for clarity. In the right side are shown the schematic representations of electron spin configurations for the quartet (Q) and doublet (D1, D2) states.

states, as depicted in Fig. 6. We have 15 allowed transitions, i.e., 15 pairs of the spin states (five within the multiplets and ten across the multiplets) with $\Delta M_S = \pm 1$ for one set of the nuclear spin configuration Eq. (7). We have simulated the hyperfine ESR spectra by superposing at most $15 \times (2I+1)^5 = 10\,935$ of the transitions. The averaged g-factor of $g = 2.007$ has been assumed. The hyperfine coupling constant of $|A_m|/g\mu_B = 1.38$ mT for the monoradical moiety has been taken from the ESR spectrum of the carboxy-TEMPO monoradical, while those for the biradical moiety is $|A_b|/g\mu_B = 0.75$ mT, being equivalent to those of the parent phenol biradical **3** [8]. The exchange interaction within the biradical moiety has been assumed to be $J(\pi)/k_B = 8.2$ K, which is the same as that found in the biradical **4**.

The simulated spectra with the line width of $\Delta B = 0.04$ mT for the Lorentzian line shape are shown in Fig. 4(b). The spectrum simulated with $|J(\sigma)/A_b| = |J'(\sigma)/A_b| = 10^4$ demonstrates the strong limit of intramolecular exchange interaction. On the other hand, the simulated spectrum of $|J(\sigma)/A_b| = |J'(\sigma)/A_b| = 10^{-3}$ is equivalent to the simple superposition of the spectra from the biradical and the monoradical, representing the weak exchange limit. The experimental spectra at room temperature are interpreted in terms of neither the strong nor the weak exchange limit. Thus, the exchange interactions between the biradical and the monoradical moieties are estimated in the same order of magnitude as the hyperfine couplings; $|J(\sigma)/A_b| \sim |J'(\sigma)/A_b| \sim 1$.

3.2.2. First-order perturbation treatments

Satisfactory agreement between the experimental and the simulated spectra, however, is not obtained, as shown Fig. 4. The disagreement suggests the fluctuation of $J(\sigma)$ and $J'(\sigma)$ due to conformational interconversion of the molecule **2** in solutions. Effects of molecular dynamics on ESR spectra in solutions have been studied for nitroxide oligoradicals with a flexible long-chain structure. Hyperfine ESR line broadenings for nitroxide biradicals have been rationalized by Luckhurst [11] on the basis of a relaxation matrix method developed by Redfield and Freed [12]. Another way of analyzing ESR line shapes affected by spin dynamics is to use a general line shape equation, which has been derived in terms of the density matrix theory in the Liouville representation [13]. Dynamical ESR spectra for biradicals have been simulated successfully [14] with the density matrix method. Effects of molecular dynamics on ESR spectra in solutions have not been studied so much for triradicals as compared with those for biradicals. ESR spectra of a triradical with three nitroxide groups have been analyzed in terms of the relaxation matrix [15] and the composite Liouville space formulation [16]. We present here an alternative approach based on perturbation treatments assuming that the exchange interaction within the biradical moiety $J(\pi)$ is much larger than those between the biradical and the monoradical moieties $|J(\sigma)|$, $|J'(\sigma)|$. This approach gives the transition assignment of specific ESR signals in complicated hyperfine splitting patterns, which is difficult to obtain by the use of the exact diagonalization described above, explaining the appearance of the triad signals for **2**.

The spin Hamiltonian Eq. (3) is split into two parts,

$$H^{(0)} = g\mu_B B(S^z_{b1} + S^z_{b2} + S^z_m) - 2J(\pi)\mathbf{S}_{b1}\cdot\mathbf{S}_{b2} \tag{8}$$

$$H^{(1)} = -2J(\sigma)\mathbf{S}_m\cdot\mathbf{S}_{b1} - 2J'(\sigma)\mathbf{S}_{b2}\cdot\mathbf{S}_m + A_b(I^z_{b1}S^z_{b1} + I^z_{b2}S^z_{b2}) + A_m I^z_m S^z_m \tag{9}$$

The unperturbed Hamiltonian $H^{(0)}$ is block-diagonalized according to the z-component of the total electron spin M_S,

$$\left(\sum_I S^z_I\right)|m^S_{b1},\ m^S_{b2},\ m^S_m,\ m^I\rangle = M^S_B|m^S_{b1},\ m^S_{b2},\ m^S_m,\ m^I\rangle \quad (M_S = \pm 3/2,\ \pm 1/2) \tag{10}$$

$$\mathbf{H}^{(0)} = \begin{bmatrix} \frac{3}{2}\mathbf{g}\mu_B\mathbf{B} - \frac{1}{2}\mathbf{J}(\pi) & \mathbf{O} & \mathbf{O} & \mathbf{0} \\ \mathbf{O} & \mathbf{H}^{(0)}_{+1/2} & \mathbf{O} & \mathbf{O} \\ \mathbf{O} & \mathbf{O} & \mathbf{H}^{(0)}_{-1/2} & \mathbf{O} \\ \mathbf{0} & \mathbf{O} & \mathbf{O} & -\frac{3}{2}\mathbf{g}\mu_B\mathbf{B} - \frac{1}{2}\mathbf{J}(\pi) \end{bmatrix} \tag{11}$$

The four block submatrices correspond to $M_S = +3/2$, $+1/2$, $-1/2$, and $-3/2$. The submatrices for $M_S = \pm 1/2$ are

$$\mathbf{H}^{(0)}_{\pm 1/2} = \begin{bmatrix} \pm\frac{1}{2}g\mu_B B + \frac{1}{2}J(\pi) & -J(\pi) & 0 \\ -J(\pi) & \pm\frac{1}{2}g\mu_B B + \frac{1}{2}J(\pi) & 0 \\ 0 & 0 & \pm\frac{1}{2}g\mu_B B - \frac{1}{2}J(\pi) \end{bmatrix} \tag{12}$$

Thus, we obtain the zeroth order energy eigenvalues and the eigenvectors. The perturbation Hamiltonian $H^{(1)}$ can be block-diagonalized as well in terms of a unitary matrix **U** which is set up with the eigenvectors of the unperturbed Hamiltonian $H^{(0)}$. The perturbed vectors $\mathbf{x}_n$ and the state energies E_n to the first order are obtained by the conventional Rayleigh-Schrödinger perturbation theory,

$$\mathbf{x}_n = \mathbf{x}_n^{(0)} + \sum_{i \neq n} \frac{H_{in}^{(1)}}{E_n^{(0)} - E_i^{(0)}} \mathbf{x}_n^{(0)} \tag{13}$$

$$E_n = E_n^{(0)} + H_{nn}^{(1)} \tag{14}$$

where $H_{in}^{(1)}$ is the matrix element of the first order submatrices. Thus:

$$\mathbf{U}^{-1}\mathbf{H}^{(1)}\mathbf{U} = \begin{bmatrix} -J(\sigma) + \frac{1}{2}[A_b(m_{b1} + m_{b2}) + A_m m_m] & \mathbf{O} & \mathbf{O} & 0 \\ \mathbf{O} & (\mathbf{U}^{-1}\mathbf{H}^{(1)}\mathbf{U})_{+1/2} & \mathbf{O} & \mathbf{O} \\ \mathbf{O} & \mathbf{O} & (\mathbf{U}^{-1}\mathbf{H}^{(1)}\mathbf{U})_{-1/2} & \mathbf{O} \\ 0 & \mathbf{O} & \mathbf{O} & -J(\sigma) - \frac{1}{2}[A_b(m_{b1} + m_{b2}) + A_m m_m] \end{bmatrix} \tag{15}$$

$$(\mathbf{U}^{-1}\mathbf{H}^{(1)}\mathbf{U})_{\pm 1/2} = \begin{bmatrix} \pm\frac{1}{2}A_m m_m & \pm\frac{1}{\sqrt{6}}A_b(m_{b1} - m_{b2}) & \mp\frac{1}{2\sqrt{3}}A_b(m_{b1} - m_{b2}) \\ \pm\frac{1}{\sqrt{6}}A_b(m_{b1} - m_{b2}) & -J(\sigma) \pm \frac{1}{6}[A_b(m_{b1} + m_{b2}) + A_m m_m] & \pm\frac{1}{3\sqrt{2}}[A_b(m_{b1} + m_{b2}) - 2A_m m_m] \\ \mp\frac{1}{2\sqrt{3}}A_b(m_{b1} - m_{b2}) & \pm\frac{1}{3\sqrt{2}}[A_b(m_{b1} + m_{b2}) - 2A_m m_m] & 2J(\sigma) \pm \frac{1}{6}[2A_b(m_{b1} + m_{b2}) - A_m m_m] \end{bmatrix} \tag{16}$$

where the two exchange interactions $J(\sigma)$ and $J'(\sigma)$ are assumed to be identical for simplicity. The nuclear spin quantum numbers in Eqs. (15) and (16) are given by

$$m_{b1} \equiv m_{b1}(1) + m_{b1}(2) \tag{17}$$

$$m_{b2} \equiv m_{b2}(1) + m_{b2}(2) \tag{18}$$

The transition field $B(i \leftrightarrow j)$ and the relative intensity $P(i \leftrightarrow j)$ associated with the ith and the jth states for the allowed ESR transition with $\Delta M_S = \pm 1$ are calculated as

$$h\nu = E(i) - E(j) \equiv \Delta E(i \leftrightarrow j) \quad (\nu\text{: the microwave frequency}) \tag{19}$$

$$\delta\Delta E(i \leftrightarrow j) \equiv \Delta E(i \leftrightarrow j) - g\mu_B B \tag{20}$$

$$B(i \leftrightarrow j) = B_0 - \frac{\delta\Delta E(i \leftrightarrow j)}{g\mu_B} \tag{21}$$

$$P(i \leftrightarrow j) = |\langle i|S_T^X|j\rangle|^2 \tag{22}$$

where S_T^X denotes the spin operator of the x-component of the total electron spin. The central field B_0 in Eq. (21),

$$B_0 = \frac{h\nu}{g\mu_B} \tag{23}$$

is the single resonance field appearing when both J and A are vanishing. We have fifteen allowed transitions with $\Delta M_S = \pm 1$, as mentioned above. Since the intramolecular exchange interaction within the biradical moiety $J(\pi)/k_B = 8$ K is much larger than all other interactions, one of the two doublet states D1 lies far apart above the other doublet (D2) and the quartet (Q) states, as depicted in Fig. 6. Therefore, we can exclude the contribution from allowed ESR transitions across the multiplets, i.e., those between D1 and Q or between D1 and D2. One has only nine pairs of states, five within the multiplets and four across the multiplets of Q and D2.

In Table 1 are listed the first-order resonance fields as measured from the central field B_0. It should be noted that the resonance field $\delta\Delta E(1 \leftrightarrow 2)/g\mu_B$ is independent of the exchange interaction $J(\sigma)$. Thus, the transition $\Delta E(1 \leftrightarrow 2)$ is little affected by the fluctuation of the $J(\sigma)$ values. Furthermore, the spacing of this transition equals to the hyperfine coupling constant of the monoradical $|A_m|$. The intense triad of the signals with the spacing of $|A_m|$ in the observed ESR spectra are assigned to the transition of $\Delta E(1 \leftrightarrow 2)$ in D1. Resonance fields of other transitions undergo a contribution of $J(\sigma)$, which fluctuates in a solution. The appearance of the intense triad signals and the rest of the broadened signals indicate that the exchange interactions through the σ-bonds are quite small as compared with that within the biradical moiety: $J(\pi) \gg |J(\sigma)|$, $|J'(\sigma)| \sim |A_b|$, $|A_m|$. The

Table 1
First-order resonance fields $B(i \leftrightarrow j) = B_0 - \delta\Delta E(i \leftrightarrow j)/g\mu_B$ of allowed ESR transitions for the Hamiltonian, Eqs. (8) and (9)[a]

$i-j$	(Multiplet)	$\delta\Delta E(i \leftrightarrow j)$[b]
1–2	(D1–D1)	$A_m m_m$
3–4	(Q–Q)	$1/4[-J(\sigma) + A_b(m_{b1} + m_{b2}) + 2A_m m_m + E_1]$
4–5	(Q–Q)	$1/4[2A_b(m_{b1} + m_{b2}) - E_1 + E_2]$
5–6	(Q–Q)	$1/4[6J(\sigma) + A_b(m_{b1} + m_{b2}) + 2A_m m_m - E_2]$
7–8	(D2–D2)	$1/4[2A_b(m_{b1} + m_{b2}) + E_1 - E_2]$
3–7	(Q–D2)	$1/4[-6J(\sigma) + A_b(m_{b1} + m_{b2}) + 2A_m m_m - E_1]$
4–8	(Q–D2)	$1/4[2A_b(m_{b1} + m_{b2}) - E_1 - E_2]$
5–7	(Q–D2)	$1/4[2A_b(m_{b1} + m_{b2}) + E_1 + E_2]$
6–8	(Q–D2)	$1/4[6J(\sigma) + A_b(m_{b1} + m_{b2}) + 2A_m m_m + E_2]$

[a] $B_0 \equiv h\nu/g\mu_B$.

[b] $m_{b1} \equiv m_{b1}(1) + m_{b1}(2)$
$m_{b2} \equiv m_{b2}(1) + m_{b2}(2)$

$$E_1 = \sqrt{36J(\sigma)^2 + 4J(\sigma)[A_b(m_{b1} + m_{b2}) - 2A_m m_m] + [A_b(m_{b1} + m_{b2}) - 2A_m m_m]^2}$$

$$E_2 = \sqrt{36J(\sigma)^2 - 4J(\sigma)[A_b(m_{b1} + m_{b2}) - 2A_m m_m] + [A_b(m_{b1} + m_{b2}) - 2A_m m_m]^2}$$

exchange interaction in the triradical **2** is truncated efficiently by the ester group and the pipelidine skeleton of TEMPO.

3.3. Magnetic susceptibility of TEMPO-substituted triradical 2

Temperature dependence of paramagnetic susceptibility χ_p of the triradical **2** is shown in Fig. 3. When the spin–spin interaction is negligible as compared with the thermal energy $k_B T$ of the room temperature, the $\chi_p T$ value is given by

$$\chi_p T = \frac{N_A g^2 \mu_B^2}{3k_B} S(S+1) \times 3 = 1.133 \text{ emu K mol}^{-1} \quad (24)$$

$$(S = 1/2, g = 2.007)$$

for 3 mol of magnetically free $S = 1/2$ spins. The experimental value agrees with Eq. (24), indicating that the purity of the triradical **2** is about 100% and that the intra and intermolecular magnetic interactions of **2** are much weaker than the thermal energy of the room temperature. As the temperature is decreased, the $\chi_p T$ value monotonically decreases, as depicted in Fig. 3. The triradical **2** does not exhibit any increase in $\chi_p T$ such as that for the biradicals **3** and **4**, indicating that the intermolecular antiferromagnetic interactions are as large as, or larger than the ferromagnetic interaction $J(\pi)$ in the biradical moiety. Provided that the intermolecular antiferromagnetic interactions are larger than $J(\pi)/k_B \sim 8$ K, a ferrimagnetic behavior of $\chi_p T$, a minimum and an upturn on lowering the temperature, should appear in the temperature range examined. The monotonic decrease in $\chi_p T$ suggests that the triradical **2** fails to make any head-to-tail molecular packing patterns as depicted in Fig. 1(c) and (d). X-ray crystal structure analysis for **2** is underway.

4. Conclusion

As part of the research of single-component organic molecule-based ferrimagnetics, we have synthesized the TEMPO-substituted triradical **2** and the cyclohexyl biradical **4**. From the magnetic susceptibility measurements for **4**, the intramolecular ferromagnetic interaction in the *m*-phenylene bis(nitronyl nitroxide) biradical is found to be retained after the esterification. The solution-phase ESR spectra of the triradical **2** have been explained by the perturbation treatment. It is shown that the exchange interaction within the biradical moiety $J(\pi)$ is much larger than those between the biradical and the monoradical moieties $|J(\sigma)|$ and $|J'(\sigma)|$. Hyperfine ESR spectroscopy in fluid solutions allows us to determine the exchange interactions, the magnitude of which is outside the range for conventional magnetic susceptibility experiments in solid states. We find that the exchange interaction in the triradical **2** is truncated efficiently by the ester group and the aliphatic pipelidine skeleton of TEMPO.

Acknowledgements

This work has been supported by Grants-in-Aid for Scientific Research from the Ministry of Education, Culture, Sports, Science and Technology, Japan.

References

[1] For reviews of molecule-based magnetics, see (a) D. Gatteschi, O. Kahn, J.S. Miller, F. Palacio (Eds.), Molecular Magnetic Materials, Kluwer Academic, Dordrecht, 1991;
(b) H. Iwamura, J.S. Miller (Eds.), Mol. Cryst. Liq. Cryst., 232–233 (1993);
(c) J.S. Miller, A.J. Epstein (Eds.), Mol. Cryst. Liq. Cryst., 271–274 (1995);
(d) K. Itoh, J.S. Miller, T. Takui (Eds.), Mol. Cryst. Liq. Cryst., 305–306 (1997);
(e) O. Kahn (Ed.), Mol. Cryst. Liq. Cryst., 334–335 (1999);
(f) O. Kahn, Molecular Magnetism, Wiley-VCH, New York, 1993;
(g) P.M. Lahti (Ed.), Magnetic Properties of Organic Materials, Marcel Dekker, New York, 1999;
(h) K. Itoh, M. Kinoshita (Eds.), Molecular Magnetism, Gordon and Breach, Amsterdam/Kodansha, Tokyo, 2000;
(i) G. Christou, Polyhedron 20 (2001) 1785.
[2] (a) M. Kinoshita, P. Turek, M. Tamura, K. Nozawa, D. Shiomi, Y. Nakazawa, M. Ishikawa, M. Takahashi, K. Awaga, T. Inabe, Y. Maruyama, Chem. Lett. (1991) 1225;

(b) M. Tamura, Y. Nakazawa, D. Shiomi, K. Nozawa, Y. Hosokoshi, M. Ishikawa, M. Takahashi, M. Kinoshita, Chem. Phys. Lett. 189 (1991) 401;
(c) Y. Nakazawa, M. Tamura, N. Shirakawa, D. Shiomi, M. Takahashi, M. Kinoshita, M. Ishikawa, Phys. Rev. B 46 (1992) 8906.
[3] A.L. Buchachenko, Dokl. Phys. Chem. 244 (1979) 107.
[4] L. Néel, Ann. Phys. (Ser. 12) 3 (1948) 137.
[5] (a) D. Shiomi, M. Nishizawa, K. Sato, T. Takui, K. Itoh, H. Sakurai, A. Izuoka, T. Sugawara, J. Phys. Chem. B 101 (1997) 3342;
(b) M. Nishizawa, D. Shiomi, K. Sato, T. Takui, K. Itoh, H. Sawa, R. Kato, H. Sakurai, A. Izuoka, T. Sugawara, J. Phys. Chem. B 104 (2000) 503;
(c) D. Shiomi, K. Sato, T. Takui, J. Phys. Chem. B 104 (2000) 1961;
(d) D. Shiomi, K. Sato, T. Takui, J. Phys. Chem. B 105 (2001) 2932;
(e) D. Shiomi, K. Sato, T. Takui, J. Phys. Chem. A 106 (2002) 2096;
(f) D. Shiomi, M. Nishizawa, K. Kamiyama, S. Hase, T. Kanaya, K. Sato, T. Takui, Synth. Met. 121 (2001) 1810;
(g) K. Kamiyama, D. Shiomi, S. Hase, M. Nishizawa, K. Sato, M. Kozaki, K. Okada, T. Takui, Appl. Magn. Reson. 19 (2000) 45;
(h) D. Shiomi, K. Ito, M. Nishizawa, K. Sato, T. Takui, K. Itoh, Synth. Met. 103 (1999) 2271.
[6] (a) D. Shiomi, M. Nishizawa, K. Kamiyama, S. Hase, T. Kanaya, K. Sato, T. Takui, Synth. Met. 121 (2001) 1810;
(b) T. Kanaya, D. Shiomi, K. Sato, T. Takui, Polyhedron 20 (2001) 1397.
[7] D. Shiomi, T. Kanaya, K. Sato, M. Mito, K. Takeda, T. Takui, J. Am. Chem. Soc. 123 (2001) 11823.
[8] S. Hase, D. Shiomi, K. Sato, T. Takui, J. Mater. Chem. 11 (2001) 756.
[9] B.D. Bleany, K. Bowers, Proc. R. Soc. London A 214 (1952) 451.
[10] D. Shiomi, C. Kaneda, T. Kanaya, K. Sato, T. Takui, Appl. Magn. Reson. 23 (2003) 495.
[11] (a) G.R. Luckhurst, Mol. Phys. 10 (1966) 543;
(b) G.R. Luckhurst, G.F. Pedulli, J. Am. Chem. Soc. 92 (1970) 4738.
[12] (a) A.G. Redfield, IBM J. Res. Develop. 1 (1957) 19;
(b) J.H. Freed, G.K. Frankel, J. Chem. Phys. 39 (1963) 326;
(c) J.H. Freed, G.K. Frankel, J. Chem. Phys. 41 (1964) 699.
[13] J. Heinzer, Mol. Phys. 22 (1971) 167.
[14] S. Sankarapandi, G.V.R. Chandramouli, C. Daul, P.T. Manoharan, J. Magn. Reson. A 103 (1993) 163.
[15] (a) A. Hudson, G.R. Luckhurst, Mol. Phys. 13 (1967) 409;
(b) A. Hudson, G.R. Luckhurst, Chem. Rev. 69 (1969) 191.
[16] C. Corvaja, M. DeMarchi, A. Toffoletti, Appl. Magn. Reson. 12 (1997) 1.